Creation of Design and Analysis Tools for Large Design Space Resuable Launch Vehicle Shape Optimization

A. Cusick* & K. Kontis†
School of Engineering, University of Glasgow, Scotland

A design optimization suite currently under development for arbitrary super-hypersonic vehicles is introduced. A brief review of literature on the subject is presented. Parameterization techniques utilized to obtain realistic geometries of various flying components are discussed. Well known engineering methods for the prediction of inviscid high speed aerodynamic coefficients are outlined, alongside implementation of streamline tracing and mesh interpolation for the calculation of viscous and local condition dependent approaches. Global optimization methods are employed, with detailed discussion on the specific characteristics chosen for this work. Validation cases are presented for the aerodynamic module, comparing computed results to wind tunnel tests gathered in previously published research. An overview of the optimization loop is provided, followed by an aerodynamic design optimization, demonstrating the potential of the combined methodologies.

I. Introduction

Current concepts for reusable launch vehicles (RLV) vary drastically in their nature. Much of this can be explained by varying mission specifications and propulsive methods. However, differing experience between institutions, and a general lack of experience with respect to hypersonic lifting vehicles, certainly contribute to this large variation. With advancements in computer technology and optimization methods, it is no longer reasonable or time effective to create an initial design based on experience, and iterate once multi-disciplinary analysis has been carried out. Instead, a design optimization approach should be employed, in which analysis can be carried out on thousands of vehicle configurations at relatively small computational cost. To do this, engineering level tools are utilized. These methods do not paint the entire picture, and can potentially produce unrealistic or poorly analyzed designs. However, if they are implemented correctly for the problem, and their limitations known in advance, they can provide meaningful results in the hands of an experienced engineer. This a priori knowledge is critical, as it will guide the algorithm to truly optimal configurations, by imposing realistic boundaries for a given vehicle component, flight regime, or mission. Furthermore, it allows the most feasible designs to be selected, perhaps through means which cannot be readily measured at the engineering level.

This paper introduces the foundations of a design optimization framework for super-hypersonic vehicles, currently under development at the University of Glasgow, which presently combines rapid aerodynamic analysis with heuristic optimization techniques. Firstly, a brief review of the state-of-the-art in super-hypersonic vehicle optimization is presented, further demonstrating the motivation behind creating and combining such a methods. Next, the specific techniques implemented in terms of vehicle generation, aerodynamic prediction, and optimization algorithms are discussed. The combination of these modules in the context of an optimization loop is then outlined, with discussion of infeasible designs and violation parameters. Validation data is provided for the employed high speed aerodynamic module, accompanied by an aerodynamic shape optimization, with a pre-existing configuration being analyzed for comparative purposes.

A. Brief Review of Super-Hypersonic Vehicle Optimization

Previous research on the topic varies drastically by discipline or disciplines considered, fidelity of analysis, optimization method, objective functions and design variables. An optimization comprising of only one disciplinary analysis may result in ideal cost function values, but can be easily deemed infeasible by an experienced engineer. Increasing the number of accurately analyzed disciplines leads to further constraints placed on the optimizer, resulting in higher cost functions, but ultimately more feasible designs. However, no such analysis to date can be considered all-encompassing, and human experience remains the predominant factor in vehicle design. Analysis fidelity and

*PhD Student, School of Engineering, University of Glasgow.
†Professor, School of Engineering, University of Glasgow.

number of design variables, constraints and objectives should be considered together based on computational resources, as well as the research scope. High-fidelity models may provide state-of-the-art results, but can also drastically increase computational cost. Couple this with the knowledge that increasing number of design variables has a large effect on the iterations required for convergence, and it is clear that limitations must be enforced from the outset.

If an existing configuration is sought to be optimized, it is reasonable to assume that the design space will be limited compared to that of a random start point design optimization; as this ensures that the optimal configuration will not vary significantly from that of the original. A close to optimal starting point makes gradient based optimization techniques coupled with high-fidelity analysis appealing, considering that a small design space may require relatively few iterations to converge. On top of this, in an optimization where only small alterations may be made to the configuration throughout, it is essential that the physics are captured as accurately as possible. Furthermore, assuming a basis design that is close to optimal exists, such an optimization may be aimed at a latter stage of the design process, where it is essential that computational resources are dedicated to state-of-the-art prediction methods.

In cases where a starting point is not available, perhaps in the early conceptual or design phases of a relatively new concept, global design optimization techniques combined with lower fidelity analysis methods are well suited to the problem. Taking full advantage of the optimization process requires a large design space, in which novel, optimal configurations can be found that may not be obvious to an experienced engineer. Utilizing a population based optimization algorithm with low-fidelity methods allows the broad search space to be explored for relatively cheap computational cost. If multiple objective functions are sought to be minimized, this approach also allows the creation of Pareto fronts, in which a set of optimal solutions are found. During the early phases of a design project, these fronts allow feasible configurations to be extracted from the results by experience, rather than being purely determined by the algorithm (single-objective optimization).

The majority of research focuses primarily on aerodynamic optimization. An early example of this is the work done by Landon et al[1], in which the low-fidelity Supersonic/Hypersonic Arbitrary Body Program[2] was used as the prediction tool. Chiba et al[3] used evolutionary algorithms along with surrogate models to provide approximate analysis, before feeding the most promising configurations to a Navier-Stokes solver. Here the goal was to optimize a wing-body reusable launch vehicle for flight states around a Mach number of unity. Four objective functions were employed in this research, relating to aerodynamic properties at various flight states. A similar method was employed by Tatsukawa et al[4], which utilized a genetic algorithm and a Navier-Stokes solver throughout, in this instance to optimize a body-only configuration. As with many hypersonic aerodynamic optimizations, L/D was used as an objective, together with zero-lift drag and RLV volume. Here a limited number of function evaluations was set, likely due to the computational requirements of the solver. Zhang et al[5] also used genetic algorithms to optimize hypersonic wings using local piston theory. Their method boasts low computational cost, however the force and moment inaccuracies when compared with higher fidelity solvers, along with piston theory being purely inviscid, show that it should only be used in the early design phases. Shen et al[6] also used a genetic algorithm, along with a simple modified Newtonian method, in optimization of the European EXPERT re-entry vehicle[7]. Again L/D was used as an objective function, alongside a reduction in optimum angle of attack. Another example of a modified Newtonian based optimization comes from the work of Sheffer and Dulikravich[8], with drag being minimized for cone and hypersonic plane configurations.

Of course, many disciplines define a feasible hypersonic vehicle. With strong couplings at play, multi-disciplinary optimization has gained increasing popularity over the years. Bowcutt[9] provides an early example of multi-disciplinary design optimization (MDO) applied to hypersonic aircraft; combining aerodynamic, propulsive, and trim analysis. Here, a small number of design variables were used to define the vehicle, once more with the goal of maximizing L/D. A further study conducted by Bowcutt[10] added trajectory analysis to the optimization process, setting range as an objective function for a full flight path. A missile configuration was studied, operating between $M = 4.5 - 7$. Being a trajectory driven problem, stability and control also factored heavily in the overall framework. Utilizing MDO in this analysis found a 46% increase in range over the initial baseline, showing the methods potential when applied successfully. It should be noted that the few decision variables in these works require many translations to produce full configurations. Generally, a continuous design space that defines the vehicle as physically as possible is desired, since it may lead to improved convergence. Dirkx and Mooij[11] coupled local-inclination aerothermodynamic methods with trim analysis, for both capsule and winged vehicles. Various realistic constraints were enforced, such as negative stability derivatives; maximum structural loading; minimum and maximum control surface deflections and angle of attack; as well as maximum heating requirements, with three geometric based objective functions being employed. Wuilbercq et al. [12] use reduced-order models to compute aero-thermal, heat protection, and propulsive characteristics, with the inclusion of mass estimation for reusable hybrid vehicles in both ascent and re-entry flight regimes. Overall performance of hypersonic vehicles is taken into account by Deng et al[13], coupling flight characteristics and geometric

performance parameters within objective functions. Recently, Di Giorgio et al. [14] introduced an aerothermodynamic design optimization framework for hypersonic vehicles. Aimed at high speed passenger aircraft, engineering level prediction methods are utilized, with potential future extension to multi-fidelity and surrogate based techniques. Much of the reasoning behind creation of their framework is akin to the presently described research, and further demonstrates the necessity of developing these methods in relation to high speed vehicles.

II. Vehicle Generation

Before configurations in a given design space can be analyzed and optimized, a reliable vehicle generator is required. Such a program must be able to not only create a vehicle from any given parameters within the design space boundaries, but consistently discretize the various shapes to a high enough level that analysis can be considered accurate. On the other hand, it is important that the variables required for creation are kept to a minimum. If there are too many design variables within the optimization, or design variables that do not have a clear and consistent effect on creation, the algorithm may not properly converge on optimal values.

Considering the above, in conjunction with present work focusing on wing-body vehicles, greater detail is given to the creation of lifting surfaces than it is to the fuselage. Defining the entire body or main fuselage by splines or a similar method in the chord-wise direction is a costly task in terms of variables required. This is due to the fact that such methods rely on a multitude of control points. Studying previous high speed wing-body vehicles, such as the X-34 and space shuttle, the main fuselage can usually be approximated with a constant cross-section shape. Considerably fewer design variables are required for such a definition in contrast to a varying shape in the chord-wise direction. Because of this, and since lifting surface optimization variables will have a much larger effect on the configurations performance as a whole, a constant cross-section shape is deemed to be a worthy trade-off for a significantly less complex design space. The nose and fore-body can also be described simply with only a few parameters, such as nose radius and z-offset from the vehicle centreline, leaving only wing and tail sections to be defined.

An arbitrary number of separate wing partitions can be used to create a single wing. Each partition is defined by five parameters: dihedral, taper ratio, trailing edge sweep, span, and two-dimensional aerofoil section. Of course an initial root chord is required, which can be an optimization variable directly, or a ratio of fuselage length. The decision to use trailing edge sweep as a design parameter instead of defining it at the quarter chord or leading edge was to ensure that control surfaces were not made ineffective by high rearward sweep or large sweep discrepancies between partitions. Such a definition may result in undesirable sweep elsewhere on the wing chord (eg. negative sweep at the leading edge), which can be easily calculated and constrained in the analysis phase.

Various methods have been considered for 2D aerofoil creation, based on versatility and ease of implementation. Initially, preloaded data files of existing aerofoils were chosen simply by an integer variable. However, this is relatively inflexible and creates discontinuities in the design space, leading to convergence issues and sub-optimal results. These existing shapes were instead used as target aerofoils in a shape optimization framework, to benchmark more continuous creation methods.

Bézier spline techniques are commonly utilized in aerodynamic shape generation, with two methods being implemented in the current framework. Both utilize two Bézier curves, and their implementation allows an arbitrary number of control points to be defined. The first method creates upper and lower splines, which define the aerofoil surfaces directly. This requires some boundaries to be set on the leading edge control points, to avoid sharp edges and ensure that surfaces merge smoothly. The second method employs a thickness and camber curve approach, where thickness distribution is added equally in the normal directions of the two-dimension camber line, creating consistent leading edge radii. It should be noted that no purely Bézier method allows for direct control over the aerofoils physical properties, since the control points affect the full curve shape, rather than acting as curve points themselves. The well known PARSEC[15] method has also been implemented, which creates 6th order upper and lower polynomials based on geometric characteristics such as maximum thickness, leading edge radius and trailing wedge angle.

Parts are discretized into triangular or quadrilateral elements, depending on user specification or choice of analysis methods. A number of techniques are available to create a model that accurately captures the features of a given configuration, thus ensuring a realistic surface is output. The most consistent approach is to specify target panel dimensions. This means that regardless of two given structure sizes, they will be discretized into similar area panels. For the special case of lifting surfaces, where generally high curvature only occurs at the leading or trailing edges, accurate discretization can be achieved by cosine or half-cosine methods. In order to analyze a full vehicle and not individual parts, lifting surfaces must be merged with the body, and any interior sections discarded. This is accomplished by simple vector plane analysis; finding which panels interfere with one another, and creating joints at these sections. On

completion, one continuous surface is output to be used for inviscid analysis. A separate component build-up method is also available for viscous methods, which will be discussed later.

Table 1 Example two partition wing design variable set used for preliminary optimization

Variable	Minimum	Maximum	Comments
Dihedral, deg.	0	20	Constant dihedral across wingspan
Chord/Taper ratio	0.1	1	Non-dimensional ratio of fuselage/prior chord length
Sweep, deg.	-20	20	Wing trailing edge sweep
Semispan, m	[2,1]	[5,5]	Wing partition semispan lengths
x_{c_2}	0.7	0.9	
x_{c_3}	0.5	0.7	
x_{c_4}	0.3	0.5	
x_{c_5}	0.1	0.3	
z_{c_1}	-0.03	0.03	
z_{c_2}	-0.1	0.1	
z_{c_3}	-0.1	0.2	
z_{c_4}	-0.05	0.2	Non-dimensional Bézier curve control
z_{c_5}	-0.05	0.2	points required for each camber and
z_{c_6}	0	0.01	thickness aerofoil curve. Any control
x_{t_2}	0.7	0.9	points not shown here are set at
x_{t_3}	0.5	0.7	constant (0 or 1) to anchor curves
x_{t_4}	0.3	0.5	
x_{t_5}	0.1	0.3	
z_{t_1}	0	0.03	
z_{t_2}	-0.05	0.1	
z_{t_3}	-0.05	0.2	
z_{t_4}	-0.05	0.2	
z_{t_5}	-0.05	0.1	
z_{t_6}	0.01	0.03	

III. Hypersonic Aerodynamic Prediction

A. Overview

To ensure the algorithm is computationally efficient, any analysis that is independent of flight regime is calculated in a pre-processing phase. This discussion is restricted to vehicle specific parameters, with any broader elements being loaded prior to the aerodynamic evaluation phase. Panel centre points where aerodynamic loads will be applied, along with panel areas are computed first. Outward facing normals are defined next, using the vectors created by panel corner vertices (triangular) or diagonals (quadrilateral). It should be noted that the method in which vehicles are generated ensures normals are calculated in an outward direction, regardless of whether they are defined by triangular or quadrilateral panels. Some panels may collapse into lines or points, these are flagged but not removed, allowing a user-friendly 2D matrix visualization of surfaces. Next interpolation weights are calculated, if necessary, between or within meshes, as these remain unchanged regardless of deformations or inclination to the flow. Finally, reference area and mean aerodynamic chord are specified, completing the pre-processing phase.

Instead of rotating the body at every angle of attack iteration in a given set of flight states, the incoming velocity vector is rotated, allowing surface normals calculated in the pre-processing phase to be used throughout. Tangency vectors however must be computed every iteration, as these are dependent on the direction of incoming flow. The inclination that a given surface has to the incoming flow is calculated as follows:

$$\theta_i = sin^{-1}(-\hat{V}_\infty \cdot \hat{n}_i) \tag{1}$$

Where θ is the inclination angle, i defines the specific panel on the surface, with $\hat{V}_\infty$ and $\hat{n}$ being the unit vectors of the freestream velocity and surface normal, respectively. In this sense, a positive angle means that the surface is inclined towards the flow, with a negative angle implying that it lies in the shadow region. Panels can then be flagged as impact, shadow or base, defining which methods will be used in calculating their aerodynamic properties. At this point streamlines can be integrated, for use in either viscous computations or shock-expansion methods. With freestream properties already defined and panel treatment flags in place, local conditions can be calculated, including viscous effects, and integrated to obtain the configurations aerodynamic performance at the defined flight state. This process is then repeated for every combination of desired angle of attack, Mach number and altitude, allowing large databases to be created with ease.

B. Inviscid Methods

At the conceptual or early design phases, flexibility and speed are desirable over high-fidelity accuracy. While Computational Fluid Dynamics (CFD) methods are state-of-the-art in aerodynamic prediction, the time required to analyze the thousands of configurations created in a typical large design space global optimization is unreasonable. On top of this, CFD is heavily reliant on discretization with respect to convergence and therefore accuracy. Designing an algorithm that can provide sufficient discretization not only of arbitrary vehicles, but of the complex flow domain presented by high speed flows, is far beyond the scope of this work.

Low-fidelity methods can provide rapid results purely based on vehicle geometry. While their accuracy is not up to CFD standards, it is more than acceptable for initial design optimizations covering a diverse population. Surface inclination methods such as Modified-Newtonian[16], oblique shock-expansion[17], and Tangent Wedge/Cone[18] were therefore chosen for this research. The latter two techniques assume an attached shock, which of course is not possible for certain Mach number and inclination angle combinations. All attached shock techniques therefore complete a check to ensure that they can be utilized in a given circumstance, with the use of a pre-loaded maximum θ-β-M database. In such cases where an attached shock is not possible, properties are calculated by the Modified-Newtonian method. This is due to Newtonian flow assuming a detached shock, and thus no inclination limits apply. In shadow regions, Prandtl-Meyer theory is utilized in a majority of cases, as it consistently provides increased accuracy over other methods. In special cases however, such as surfaces whose normals point in a similar direction to the freestream velocity vector (base regions); surfaces with a large expansion angle with respect to their previous panels; or in very high Mach number cases, different techniques must be applied. Here either Gaubeaud's base pressure formula[19], which is constant for a given flight state, or the assumption of shadow region Newtonian flow (freestream conditions) is used. Once again checks are put in place to ensure these special cases are treated appropriately, for example setting all panels with an inclination $\theta < -45°$ to base pressure.

To ensure rapid and accurate calculation of Prandtl-Meyer and oblique shock angles, Brent's algorithm is employed[20]. Fast searching algorithms have also been experimented with, however their speed is of course dependent on the level of discretization used to generate lookup tables, risking a drop in accuracy for reduced computational load.

C. Streamline Tracing

Streamline tracing serves two purposes in high speed aerodynamic computations, with both viscous effects and the Shock-Expansion method requiring knowledge of the flow structure on the body, making it a powerful tool in increasing the accuracy of results. Given an inviscid flow field over the entirety of a given surface, streamlines are traced from the leading edge upstream until an edge or stagnation point is reached. This process is repeated until it is known for every panel, which panel or edge it expands or contracts into. To ensure that the streamlines remain constrained to the surface, tracing is performed in two-dimensions, with the third being defined by the corresponding value that lies on the panel plane.

Since the inviscid inclination methods do not provide information on the velocity vector of the upstream flow on a panels surface, a simple yet widely used assumption is employed:

$$\vec{V}_{surface} = \hat{n} \cdot \vec{V}_{\infty} \cdot \hat{n} \tag{2}$$

Where $\vec{V}_{\infty}$ is the freestream velocity, $\hat{n}$ is the outward facing unit surface normal, and $\vec{V}_{surface}$ is the tangency velocity vector on the surface. This vector is calculated at the centre of each panel, and thus a method to provide a velocity field encompassing all corners of the surface is required. Once the flow field has been defined, a fourth order runge-kutta method is used to trace streamlines, with velocity being interpolated within individual panels. Tracing continues bound to the current panel surface until an edge is reached, where the new panel is determined and the process repeats. To ensure all panels are planar, a triangular surface is required, meaning that quadrilateral definitions will be automatically subdivided. In this form, barycentric interpolation can be utilized, allowing an accurate surface velocity to be calculated anywhere within a given panel.

D. Mesh Interpolation

Information exchange within or between meshes is a common necessity in single or multi-disciplinary analysis, thus requiring implementation of a robust and versatile method. Radial basis function (RBF) interpolation[21] has been successfully utilized in the aerospace field, particularly in cases where aero-structural coupling is sought[22, 23]. The problem is formulated as follows:

$$s(\mathbf{x}) = \sum_{j=1}^{N} \alpha_j \phi(||\mathbf{x} - \mathbf{x}_j||) + p(\mathbf{x}) \tag{3}$$

In this instance, $s(\mathbf{x})$ is the function at $\mathbf{x}$, j depicts the centre or node within the mesh, with N being the total number of nodes. The function ϕ represents a radial function with respect to Euclidean distance. Many options are available for this function, which can be found in[23]. By setting $p(\mathbf{x})$ as a linear polynomial, the interpolation does not change, regardless of translation or rotation of the mesh. Coefficients α_j are defined by the interpolation conditions:

$$s(\mathbf{x}_j) = y_j, 1 \leq j \leq N \tag{4}$$

Where y is the known positions of the centres or nodes. With the inclusion of the polynomial in equation 3, a second requirement states that:

$$\sum_{j=1}^{N} \alpha_j q(\mathbf{x}_j) = 0 \tag{5}$$

For all polynomials q equal to or lesser degree than that of p. Importantly, this ensures that the total information transfer is equal within or between meshes, making it a conservative approach. In the presented work, only single mesh interpolation has been carried out; that is aerodynamic surface centre velocity to aerodynamic surface corner point velocity. However, considering that the method can be easily applied to aero-structural coupling, which is of interest in the current research, the radial basis function interpolation provides an ideal approach that is both consistent and conservative.

E. Skin-Friction Drag

Two methods can be selected to calculate the skin-friction contribution to the overall drag coefficient. The first uses a strip theory approach similar to that implemented by Jazra and Smart[24], with the second utilizing previously integrated streamlines. A component build-up method is used, which is particularly necessary in the utilization of streamlines, as large discontinuities across components may result in inaccurate surface velocity interpolation. Both seek to compute local panel conditions, resulting in a skin-friction coefficient for each element, rather than a single full-body estimate. The main difference between these methods is thus in their calculation of characteristic length, defined from leading edge to panel. This is determined either by distance travelled along the strip in which the panel resides to its centre, or total streamline length at the exit point of the panel. The strip method allows viscous effects to be computed without streamline tracing, which decreases computational load significantly. Of course, a certain degree of accuracy may be lost, especially in high angle of attack cases. In either instance, an improved version[25] of Eckert's reference temperature method[26] is employed, along with the assumption of an adiabatic wall[27]. Options are available for laminar and turbulent flows, however at present this characteristic is user-defined, not calculated. Since

this approximate method is based on two-dimensional flat plate flow, it is important that special treatment is given to conical surfaces, as viscous forces are increased due to decreased shock effects in three-dimensions. Once again specific treatment varies depending on the flow regime, with the constant Mangler fraction being applied in laminar flow, and van Driest's turbulent cone rule being utilized otherwise[28].

IV. Optimization

A. Methodology

Optimization continues to grow in popularity across all forms of engineering, especially in early design phases. Generally this is because the analysis techniques at this stage can be approximate and therefore rapid. This means huge numbers of designs can be tested, with the end goal to find an ideal solution (single-objective) or a collection of ideal solutions known as a Pareto front[29] (multi-objective). The main issue facing such a problem is therefore deciding how to manipulate the process to find these optimal solutions, and do so in as few iterations (or cost function evaluations) as possible. In early phases, the design space is usually broad and may contain discontinuous variables, thus making gradient-based optimization techniques unsuitable. Heuristic algorithms on the other hand are designed for such problems, and while they are not mathematically guaranteed to find the global optimum for a given problem, they are considerably more efficient and versatile than other methods. The decision of which heuristic method to use was quickly narrowed down to the well-known genetic algorithm (GA)[30], and the particle swarm optimization (PSO)[31], which has gained popularity dramatically in recent years.

Many papers have shown particle swarm to be an improvement over the GA in terms of efficiency and optimal values found[32–35]. On top of this, PSO algorithms have been updated to include characteristics found in evolutionary methods, such as mutation and ageing[36, 37]. For these reasons, it was decided that the particle swarm optimizer was the superior option, with the ability to incorporate most of the techniques found in genetic algorithms.

This work looks to incorporate multiple cost functions in a single simulation, while analyzing a broad design space. Thus the selection of PSO optimizer is of paramount importance, not only to ensure faster convergence, but to provide a diverse set of globally optimal solutions. The specific methodology adopted here is a variation of the OMOPSO algorithm[36], which was chosen due to its superior performance against other multi-objective algorithms[35]. In a given optimization loop, optimality is defined by non-dominated solutions, which fill the Pareto front until a user-defined maximum is reached. Above this limit, Pareto front solutions are defined by crowding distance. Here, optimal particles are compared to their closest neighbours on the front in terms of cost function values, with the most similar solutions being discarded. Mutation is also implemented, with the swarm subdivided into three sets of equal size, and each subset having a different mutation scheme applied (no mutation, uniform mutation, non-uniform mutation).

The selection of global best plays a pivotal role in any PSO algorithms efficiency. Along with the best position that a given particle has experienced in terms of cost function, the global best defines which design variable sets that the swarm will tend towards during the current iteration. The previously described mutation and crowding distance techniques promote diversity within the swarm, and the selection of global best continues in this vein. Pareto front solutions are ranked by the number of particles that they dominate in the current iteration. Where dominance is defined by one solution having at least equal cost function values in all dimensions compared to another, with one or more of the cost function values being lesser. Particles with the highest dominating rank are often the most crowded, and selecting them as the global best can localize the search to a small section of the Pareto front. On the other hand, selecting Pareto front particles with the lowest dominating rank (those that lie on the extremities in each dimension), can ensure that a search remains sufficiently diversified, but may lack the convergence characteristics of the former method. Thus in this work, both approaches have been implemented, with either half of the population consistently selecting a high or low dominating global best throughout the optimization. In both cases, the decision of the global best particle for a given iteration should not be defined purely the highest or lowest number of dominated particles. Instead, a roulette wheel technique has been implemented, giving a particles with desirable dominance characteristics a higher chance of selection.

It should be noted that while Particle Swarm Optimization has been chosen for this work, a Genetic Algorithm has also been implemented into the framework. This allows continued comparison and increased confidence that the obtained results are in fact optimal. Additionally, future problems may be suited to a structured gene based algorithm, such as those involving multiple options for tailplane composition.

B. Design Loop

Initialization of the problem is completed as follows. Firstly, the structures to be included in the optimization are defined, allowing the correct set of design variables to be loaded. Differing variable sets exist for the available aerofoil creation methods, and thus must also be defined if they are to be included in the optimization. Angle of attack, Mach number, and altitude at which results are to be acquired must be stated. Multiple flight states are allowed, and either sequentially computed, or every combination of these three parameters can be analyzed. Disciplines to be included and analysis methods used are introduced next, along with objective functions and constraints. Problem specific parameters are loaded, such as maximum oblique-shock tables. The optimization technique is chosen; both particle swarm and genetic algorithm solvers are available. A baseline configuration can then be specified, which will be passed to the analysis phase, and its results can be used to constrain the configurations created throughout the design optimization process. Variables are defined next, along with their minimum and maximum boundaries, and any transformations that must take place before they can be passed to the vehicle generator. Many optimization variables are available to define the various parts of the vehicle, however in many circumstances, parameters may be fixed due to physical requirements or research scope. In such cases, the option is available to hold properties constant, assigning them user-defined standard values, or those of the baseline configuration.

Following initialization, the problem is passed to the selected optimizer. Before any analysis can be completed on the population, any constraints or transformations must be performed on the design variables. Constraining the configuration at the input stage allows undesirable or infeasible characteristics to be removed before they are transferred to the cost function, reducing the design space and computational expense. Some constraints are not enforceable during the input phase, and require further information provided by analysis of the configuration. The method used to impose these constraints is discussed in the proceeding paragraph. Transformations are applicable when a variable is dependent on one or more other variables, ensuring all inputs are provided to the analysis phase as physical properties.

Once the population has been constrained and any variable dependencies have been computed, the configurations can be analyzed, with their objective fitness values output. Initially, all costs are set to infinity, as certain problem set-ups can produce infeasible designs that cannot be analyzed. In scenarios where a successful design has been created and analyzed, these values will be replaced. However in the case of an infeasible design, the cost function is terminated early, resulting in an infinite cost for the given set of design parameters. As mentioned previously, the user may wish to place constraints on the optimization that can only be enforced after the analysis phase is complete. These may be relative to a baseline configuration; for example a requirement may be that the total wing area cannot be less than that of the baseline. Another example may be that negative stability derivatives are desired for a given flight state. For cases in which a configuration violates these given constraints, an exponential based penalty function is used, and its result is added to the configurations cost function values.

V. Results

A. Aerodynamic Validation

Before the aerodynamic module can be integrated into an optimization framework, it is critical that it has been shown to produce accurate results, and that any limitations are known. To do this, comparative analysis should be carried out on existing data found in literature. Here, such investigations are presented for six analytically defined body shapes, for which wind tunnel experiments were carried out by Landrum & Babb[38]. Two of the bodies replicated for this task are shown in Fig. 1. Here, a total of 2000 panels make up each configuration. Note that a half-cosine spacing method has been employed, ensuring that the areas with highest curvature (nose) are properly captured. Usually, the aerodynamic module defines atmospheric values are defined by a set altitude. However, in cases where wind tunnel data is used for validation, the actual test case flow conditions provided in the references are input.

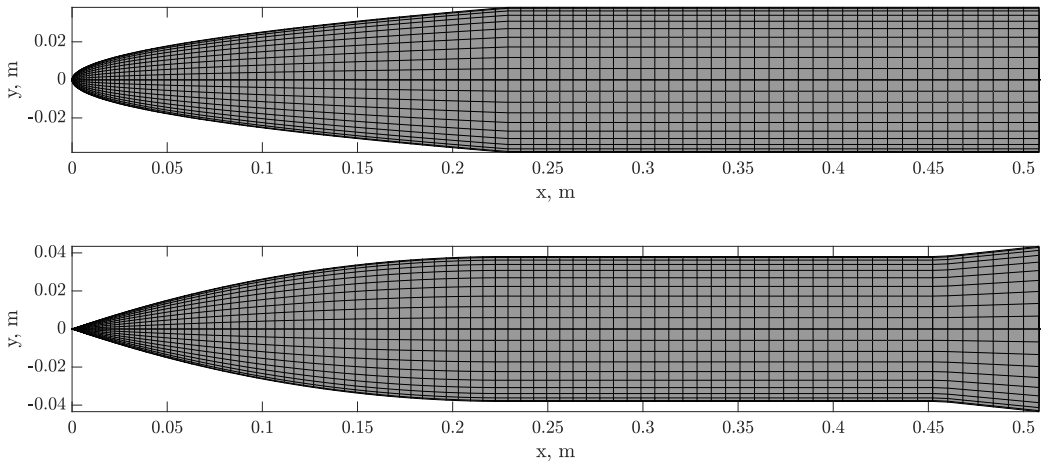

Fig. 1 Nose-body shapes modelled by vehicle generator to compare with wind tunnel data (cases 3 & 6) [38]

Two inviscid methods were utilized in these validation cases: Modified-Newtonian and Tangent Cone on impact surfaces, with Prandtl-Meyer expansion used for shaded regions in both circumstances. Figures 2 & 3 show a comparison of results for the Mach 4.63 case, with tables 2 & 3 displaying mean absolute error across the angle of attack range. It is important that the relative scale of the three aerodynamic properties shown in the figures have been taken into account before comparisons are drawn, as this may lead to incorrect assumptions about the overall accuracy of the methods displayed. Now, considering the results as a whole, it is clear that the axial force component is most accurately computed for both methods and all six cases, in terms of mean absolute error, followed by normal axial component for the Newtonian method, and pitching moment for the Tangent Cone approach.

In the majority of cases, Newtonian/Prantl-Meyer provides an accurate comparison for normal and axial forces. For configurations 2-6, there is a tendency for the normal component to be under-predicted as angle of attack increases. On the other hand, axial force is over-predicted at low inclination angles (with exception to configuration 5), falling towards or below the experimental data as inclination with respect to freestream flow is increased.

As mentioned, axial force prediction for the Tangent Cone/Prandtl-Meyer method is also shown to be relatively accurate in comparison to the test cases. In fact, for configurations 1-3, this method outperforms its Newtonian counterpart in almost every instance, with a clear reflection of the experimental data trends. However, there is a large over-prediction of normal force as angle of attack increases (or under-prediction as it decreases below zero). This can be seen across all configurations, resulting in a mean absolute error greater than ten times that of the Newtonian method in certain cases.

The discrepancies discussed are once again demonstrated in the prediction of pitching moment coefficient (measured from the nose). The Modified-Newtonian method generally over-predicts the experimental data, while the Tangent Cone approach represents a scaled-up prediction of the data with respect to angle of attack.

Configuration 6 demonstrates a particularly interesting case due to its flare structure at the rear (shown in Fig. 1). While this is not of particular interest in the presented research, this configuration produces polarizing results across the two methods. Most notably, both approaches significantly over-predict the axial force component with respect to any other configuration. Normal force and pitching moment coefficients show significantly higher error in the Newtonian case also, whereas the Tangent Cone method performs best here in terms of C_N & C_m. This is perhaps due to the attached shock introduced by the flare being appropriately captured on the impact side by the latter method. However, errors remain relatively high for the case, and further investigations required for parties interested in similar structures.

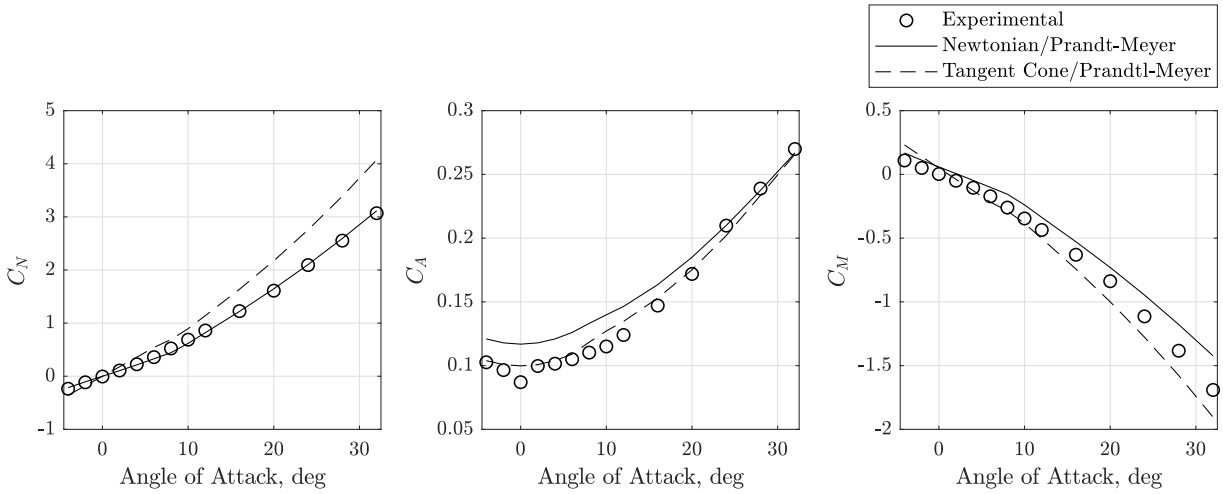

a) Numerical comparison with experimental data for configuration 1

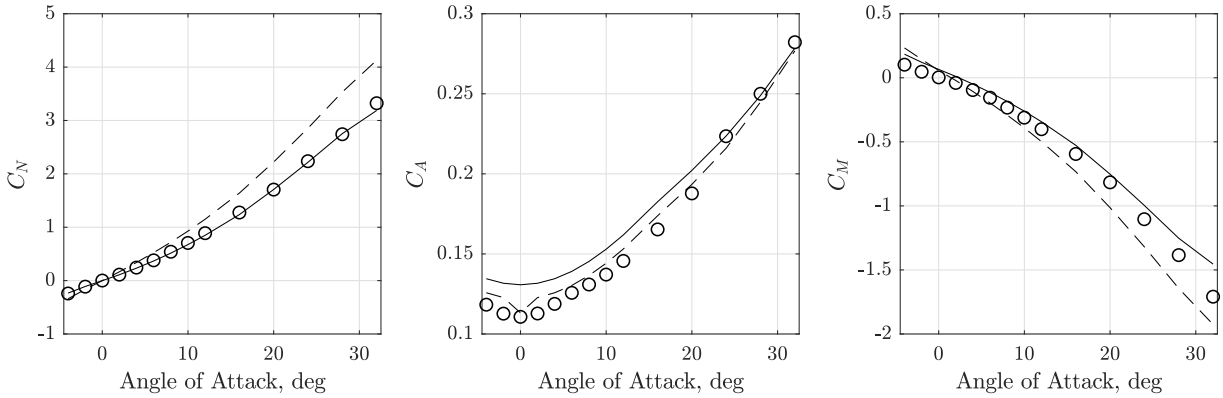

b) Numerical comparison with experimental data for configuration 2

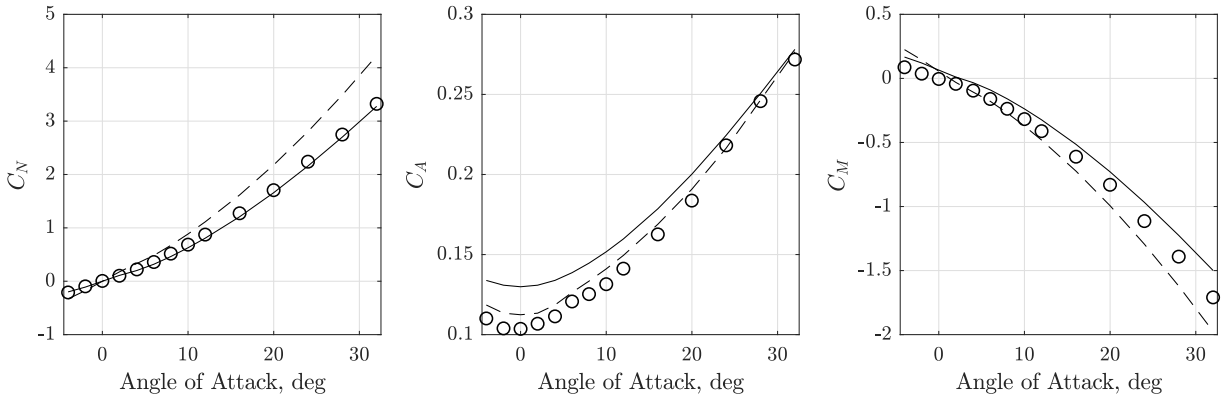

c) Numerical comparison with experimental data for configuration 3

Fig. 2 Numerical results compared to experimental data for body shapes 1-3 at Mach 4.63[38]

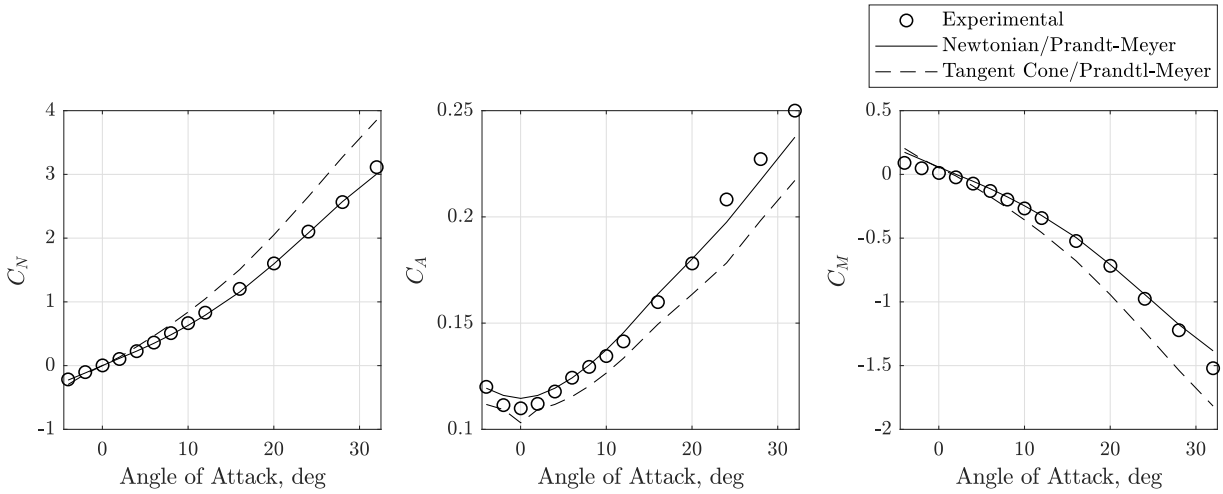

a) Numerical comparison with experimental data for configuration 4

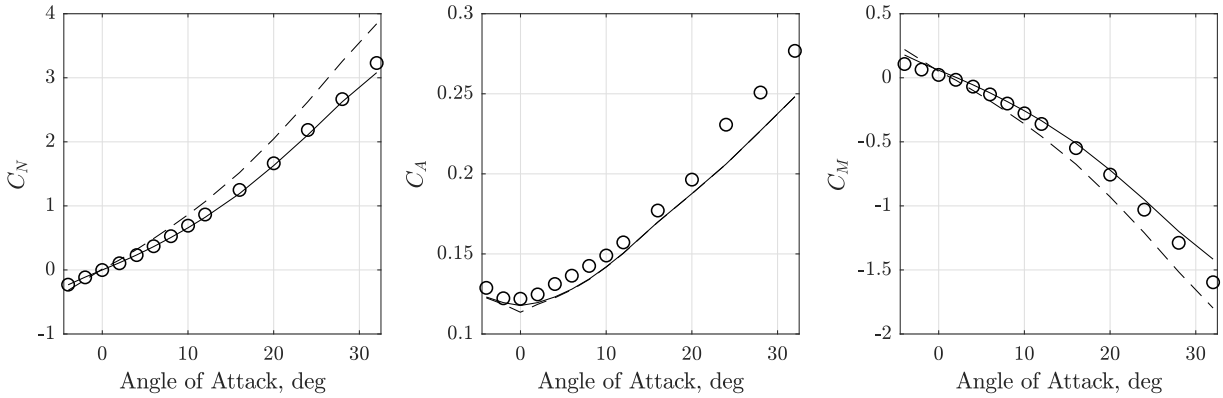

b) Numerical comparison with experimental data for configuration 5

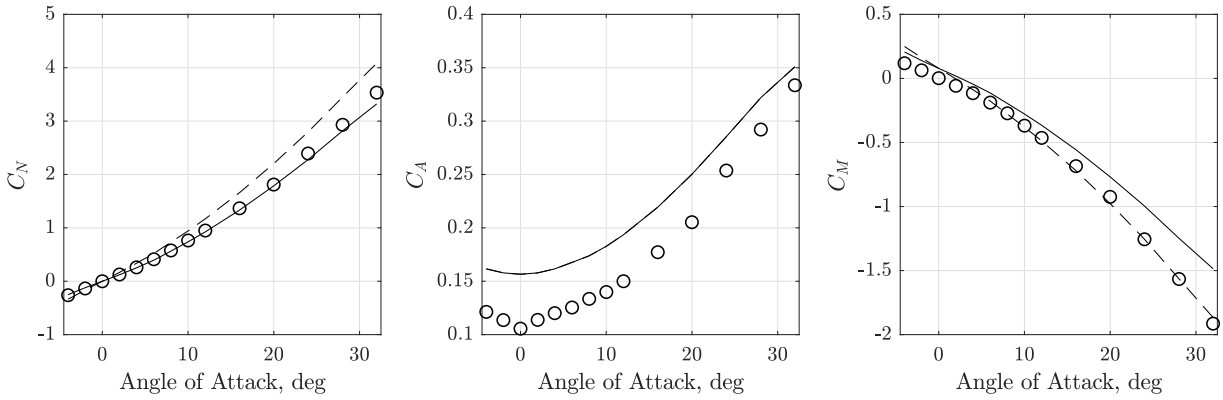

c) Numerical comparison with experimental data for configuration 6

Fig. 3 Numerical results compared to experimental data for body shapes 4-6 at Mach 4.63[38]

Table 2 Mean absolute error for Modified-Newtonian/Prandtl-Meyer computed coefficients against experimental data for $M = 4.63$, $\alpha = -4^\circ$ to 32°

Body	C_N	C_A	C_m
1	0.0288	0.0166	0.1086
2	0.0246	0.0133	0.0814
3	0.0405	0.0178	0.0989
4	0.0243	0.0045	0.0406
5	0.0343	0.0106	0.0489
6	0.0439	0.0397	0.1442

Table 3 Mean absolute error for Tangent Cone/Prandtl-Meyer computed coefficients against experimental data for $M = 4.63$, $\alpha = -4^\circ$ to 32°

Body	C_N	C_A	C_m
1	0.3366	0.0059	0.0938
2	0.2998	0.0067	0.1153
3	0.2949	0.0066	0.1038
4	0.2566	0.0126	0.1306
5	0.2301	0.0113	0.1039
6	0.2176	0.0397	0.0412

B. Preliminary Optimization Results

With the aerodynamic module showing satisfactory results for an array of configurations, an aerodynamic shape optimization was performed. Designs created throughout the simulation were compared to that of a pre-existing reusable launch vehicle concept, to show the capability of the developed framework as a whole. Here, the previously described modules: design, analysis, and optimization, are implemented into a single simulation. An inviscid wing only design optimization is carried out using the X-34[39] as a baseline configuration, with Fig. 4 displaying the overall wing-body structure. The flow conditions are equal to that of the Mach 2 experiment conducted by Brauckmann[40], with multiple cases being considered for angles of attack -5° to 20°. The optimization problem is defined as follows:

$$
\begin{aligned}
\text{minimize} \quad & -\bar{C_L}, \bar{C_D} \\
\text{subject to} \quad & \bar{L} \geq \bar{L}_{base} \\
& b \leq b_{base} \\
& 0^\circ \leq \Lambda_{LE} \leq 80^\circ \\
& \bar{M}_{root} \leq \bar{M}_{baseroot} \\
& max(t_{wing}) \leq max(t_{basewing}) \\
& max(\Delta CoP) \leq max(\Delta CoP_{base})
\end{aligned}
$$

In this instance two functions are used to define optimality: mean lift and mean drag coefficients across the defined angle of attack range. Clearly these could be combined as a single objective function. However, as previously mentioned, the methods employed are not all-encompassing, and in reality various fields define optimality. Thus it is preferable to generate a diverse Pareto front of optimal designs which can be visualized and analyzed by experienced engineers, rather than a single aerodynamically optimal configuration. In order to avoid any undesirable characteristics, and thus ensure that optimal designs found by the optimizer have an increased likelihood of being feasible, a variety of constraints have been put in place, with many coming directly from the baseline configuration. Since optimization of non-dimesionalized parameters could result in wings that are extreme in size (both small and large), Pareto front designs must have equal to or greater overall lift than the baseline; along with equal to or lower span, maximum wing thickness, and bending

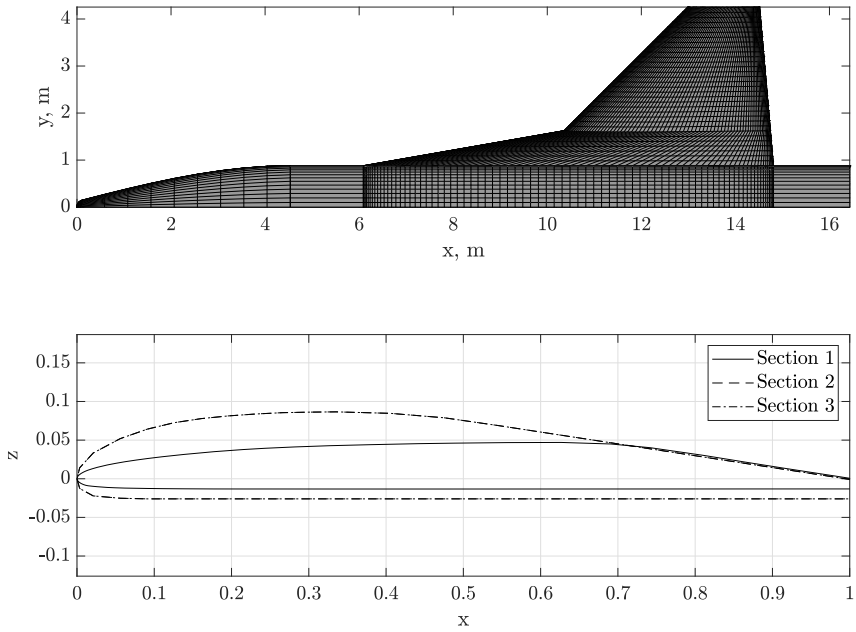

Fig. 4 X-34 wing-body & aerofoil sections (root to tip) modelled by vehicle generator

moment at the root. On top of this, it is desirable for configurations to have a low change in centre of pressure across the angle of attack range, as well as boundaries placed on leading edge sweep, for stability reasons.

The Pareto front is shown in Fig. 5. This simulation was run with 150 particles for 500 iterations, and a maximum Pareto front population of 100. In this instance, 89 optimal solutions were found, which outperform the X-34 configuration in terms of lift and/or drag coefficient, while also adhering to the constraints discussed above. Some examples of these configurations, along with their two-dimensional aerofoil shapes (from root to tip) are shown in Figs. 6 - 8. Interestingly, the optimizer appears to have taken advantage of the aerofoil shape generator, and produced some undesirable traits, such as thick trailing edges and consistently thin aerofoils with a high degree of camber. Future work will seek to eradicate this phenomena, however it is important to note that any shape generator should be able to create a high percentage of pre-existing configurations, before being utilized in an optimization framework. Altering the boundaries due to optimization results alone may lead to a generator that has been over-constrained, and cannot create readily available geometries. Instead, quantifying undesirable characteristics and handling them appropriately should be of paramount importance.

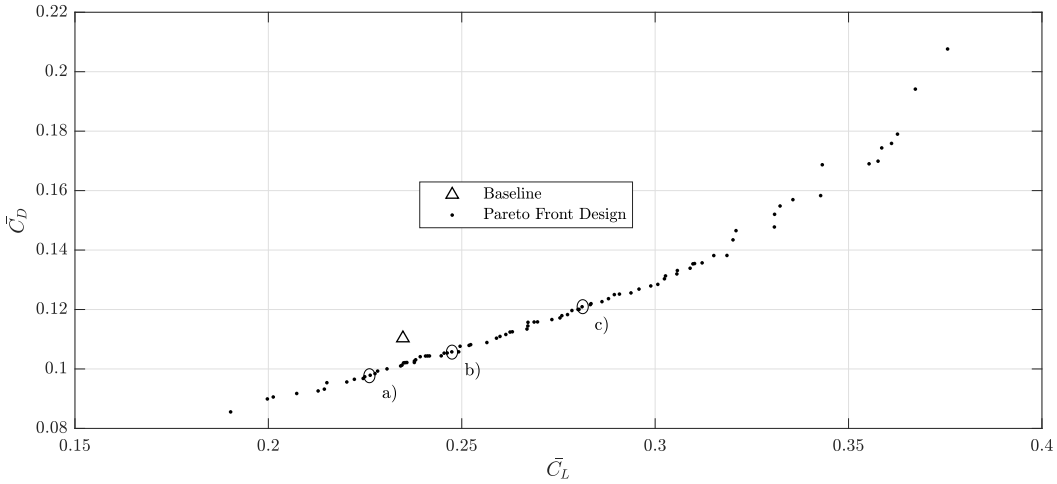

Fig. 5 Wing design optimization Pareto front, with comparative baseline configuration

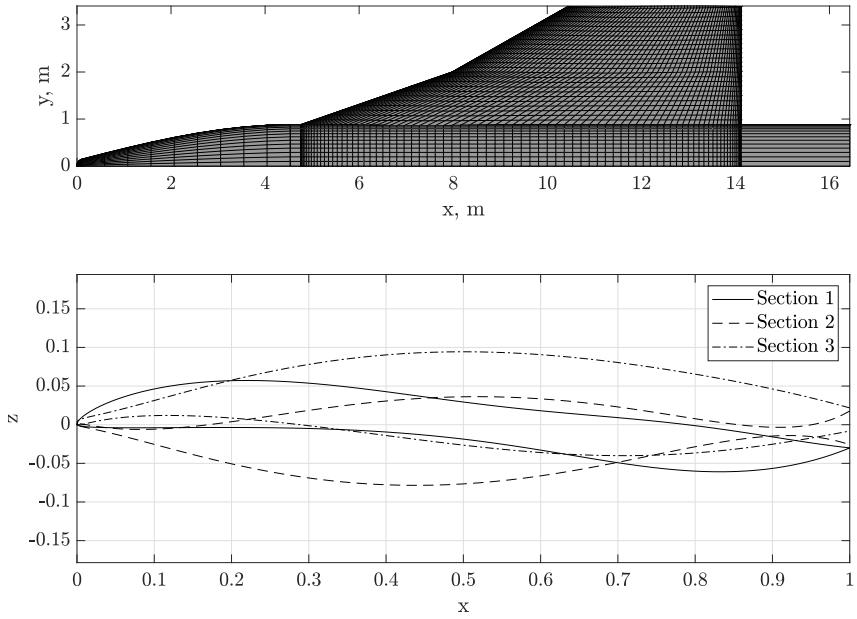

Fig. 6 Optimal configuration and non-dimensionalized aerofoil section shape for Pareto front solution a)

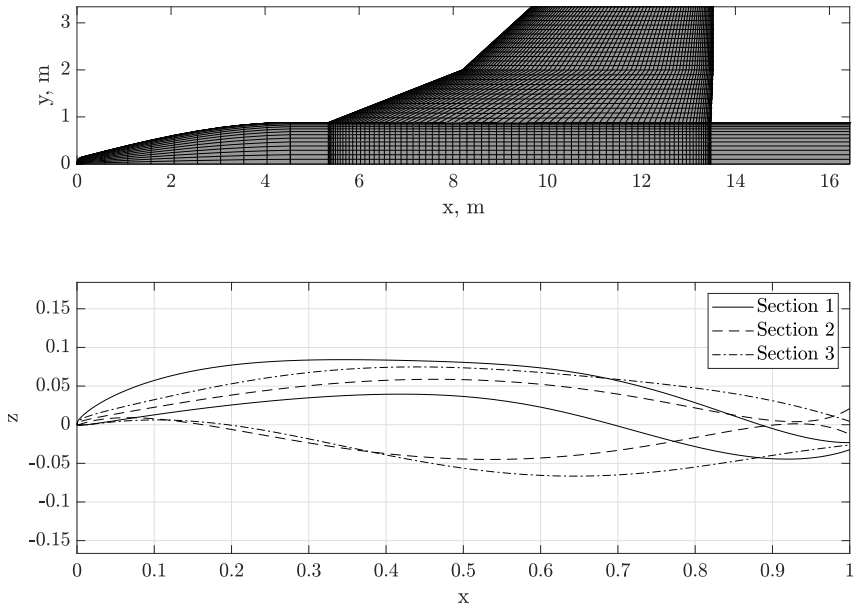

Fig. 7 Optimal configuration and non-dimensionalized aerofoil section shape for Pareto front solution b)

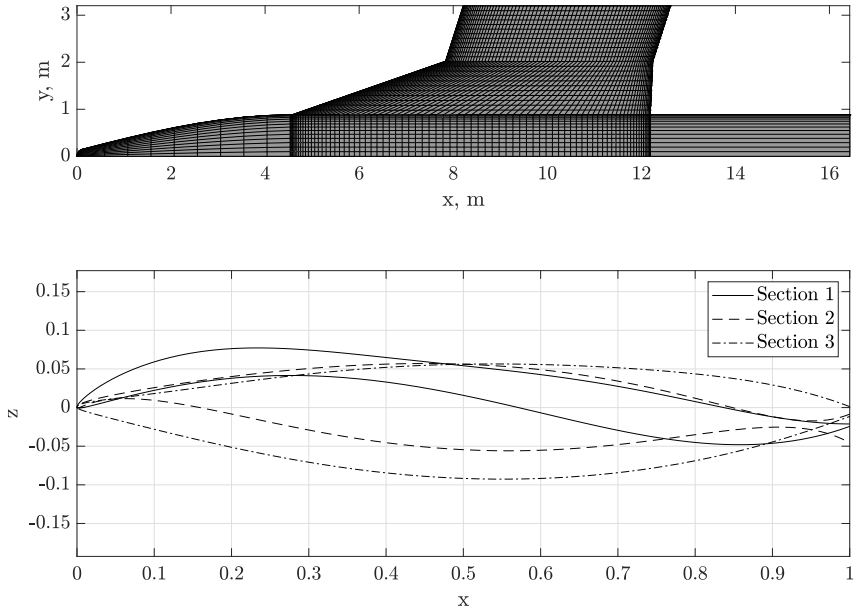

Fig. 8 Optimal configuration and non-dimensionalized aerofoil section shape for Pareto front solution c)

VI. Concluding Remarks

The aim of this paper was to introduce a global design optimization framework that is currently under development for arbitrary super-hypersonic vehicles. A vehicle generator has been presented, with a focus on versatility, to ensure that infeasible or undesirable configurations are flagged and dealt with appropriately. In terms of analysis, a low-fidelity, computationally efficient high speed aerodynamics module has been implemented. Various surface inclination methods have been included for inviscid calculations, with the option to specify separate approaches for differing vehicle components or individual panel orientations with respect to the freestream flow. Streamline integration alongside mesh interpolation have been successfully included for viscous and shock-expansion methods. An overview of the specific design optimization architecture has been provided, along with description and justification of the adopted multi-objective algorithm utilized. Validation of the aerodynamics methods has been shown, with further comparisons to existing data in literature and internal CFD computations to be carried out. Finally, an aerodynamic shape optimization was conducted, seeking to improve upon an existing wing-body configuration. Future work will look to extend the capabilities of the framework to multi-disciplinary optimization. Particular focus is on thermal and structural effects.

References

[1] Landon, M., Hall, D., Udy, J., and Perry, E., "Automatic supersonic/hypersonic aerodynamic shape optimization," *12th Applied Aerodynamics Conference*, Fluid Dynamics and Co-located Conferences, American Institute of Aeronautics and Astronautics, 1994.

[2] Gentry, A. E., Smyth, D. N., and Oliver, W. R., "The Mark IV Super-Hypersonic Arbitrary Body Program, Volume II Program Formulation," Tech. rep., Douglas Aircraft Company, Long Beach, California, 1973.

[3] Chiba, K., Obayashi, S., Nakahashi, K., Giotis, A. P., and Giannakoglou, K. C., "Design Optimization of the Wing Shape for the RLV Booster Stage Using Evolutionary Algorithms and Navier-Stokes Computations on Unstructured Grids," *International Congress on Evolutionary Methods for Design, Optimization and Control with Applications to Industrial Problems*, edited by G. Bugeda, J. Désidéri, J. Periaux, M. Schoenauer, and G. Winter, EUROGEN, Barcelona, 2003.

[4] Tatsukawa, T., Nonomura, T., Oyama, A., and Fujii, K., "Aerodynamic Design Exploration for Reusable Launch Vehicle Using Genetic Algorithm with Navier Stokes Solver," *Transactions of the Japan Society for Aeronautical and Space Sciences, Aerospace Technology Japan*, Vol. 10, No. ists28, 2012, pp. Pe_55–Pe_63.

[5] Zhang, Q., Ye, K., Ye, Z.-Y., and Zhang, W.-W., "Aerodynamic Optimization for Hypersonic Wing Design Based on Local Piston Theory," *Journal of Aircraft*, Vol. 53, No. 4, 2016, pp. 1065 – 1072.

[6] Shen, Y., Huang, W., tian Zhang, T., and Yan, L., "Parametric modeling and aerodynamic optimization of EXPERT configuration at hypersonic speeds," *Aerospace Science and Technology*, Vol. 84, 2019, pp. 641–649.

[7] Massobrio, F., Viotto, R., Serpico, M., Sansone, A., Caporicci, M., and Muylaert, J.-M., "EXPERT: An atmospheric re-entry test-bed," *Acta Astronautica*, Vol. 60, No. 12, 2007, pp. 974–985.

[8] Sheffer, S., and Dulikravich, G., "Constrained optimization of three-dimensional hypersonic vehicle configurations," *31st Aerospace Sciences Meeting*, American Institute of Aeronautics and Astronautics, 1992.

[9] Bowcutt, K., "Hypersonic aircraft optimization including aerodynamic, propulsion, and trim effects," *4th Symposium on Multidisciplinary Analysis and Optimization*, American Institute of Aeronautics and Astronautics, 1992.

[10] Bowcutt, K. G., "Multidisciplinary Optimization of Airbreathing Hypersonic Vehicles," *Journal of Propulsion and Power*, Vol. 17, No. 6, 2001, pp. 1184–1190.

[11] Dirkx, D., and Mooij, E., "Optimization of entry-vehicle shapes during conceptual design," *Acta Astronautica*, Vol. 94, No. 1, 2014, pp. 198–214.

[12] Wuilbercq, R., Pescetelli, F., Mogavero, A., Minisci, E., and Brown, R. E., "Robust multidisciplinary design and optimisation of a reusable launch vehicle," *19th AIAA International Space Planes and Hypersonic Systems and Technologies Conference*, 2014.

[13] Deng, F., Jiao, Z.-H., Chen, J., Zhang, D., and Tang, S., "Overall Performance Analysis–Oriented Aerodynamic Configuration Optimization Design for Hypersonic Vehicles," *Journal of Spacecraft and Rockets*, Vol. 54, No. 5, 2017, pp. 1015–1026.

[14] Di Giorgio, S., Quagliarella, D., Pezzella, G., and Pirozzoli, S., "An aerothermodynamic design optimization framework for hypersonic vehicles," *Aerospace Science and Technology*, Vol. 84, 2019, pp. 339–347.

[15] Sobieczky, H., "Parametric Airfoils and Wings," *Recent development of aerodynamic design methodologies*, Springer, 1999, pp. 71–87.

[16] Jaslow, H., "Aerodynamic relationships inherent in Newtonian impact theory," *AIAA Journal*, Vol. 6, No. 4, 1968, pp. 608–612.

[17] Eggers, A. J., "The Generalized Shock-Expansion Method and Its Application to Bodies Traveling at High Supersonic Air Speeds," *Journal of the Aeronautical Sciences*, Vol. 22, No. 4, 1955, pp. 231–238. doi:10.2514/8.3316.

[18] Dejarnette, F. R., Cheatwood, F. M., Hamilton, H. H., and Weilmuenster, K. J., "A review of some approximate methods used in aerodynamic heating analyses," *Journal of Thermophysics and Heat Transfer*, Vol. 1, No. 1, 1987, pp. 5–12.

[19] Guidi, A., Chu, Q. P., Mulder, J. A., and Buursink, J., "Implementation of an Aerodynamic Toolbox in a Reentry Flight Simulator," *Journal of Spacecraft and Rockets*, Vol. 40, No. 1, 2003, pp. 138–141.

[20] Press, W. H., Teukolsky, S. A., Vetterling, W. T., and Flannery, B. P., *Numerical Recipes in C*, 2nd ed., Cambridge University Press, 1988.

[21] Broomhead, D. S., and Lowe, D., "Radial basis functions, multi-variable functional interpolation and adaptive networks," Tech. rep., Royal Signals and Radar Establishment Malvern (United Kingdom), 1988.

[22] Beckert, A., and Wendland, H., "Multivariate interpolation for fluid-structure-interaction problems using radial basis functions," *Aerospace Science and Technology*, Vol. 5, No. 2, 2001, pp. 125–134.

[23] Rendall, T. C. S., and Allen, C. B., "Unified fluid–structure interpolation and mesh motion using radial basis functions," *International Journal for Nmuerical Methods in Engineering*, Vol. 74, 2008, pp. 1519–1559.

[24] Jazra, T., and Smart, M., "Development of an Aerodynamics Code for the Optimisation of Hypersonic Vehicles," *47th AIAA Aerospace Sciences Meeting*, 2009.

[25] Meador, W. E., and Smart, M. K., "Reference Enthalpy Method Developed from Solutions of the Boundary-Layer Equations," *AIAA Journal*, Vol. 43, No. 1, 2005.

[26] Eckert, E., "Engineering relations for heat transfer and friction in high-velocity laminar and turbulent boundary-layer flow over surfaces with constant pressure and temperature," *Transactions of the ASME*, Vol. 78, No. 6, 1956, pp. 1273–1283.

[27] Anderson, J., *Hypersonic and High-Temperature Gas Dynamics*, 2nd ed., American Institute of Aeronautics and Astronautics, 2006.

[28] van Driest, E. R., "The Problem of Aerodynamic Heating," *Aeronautical Engineering Review*, 1956, pp. 26–41.

[29] Van Veldhuizen, D. A., and Lamont, G. B., "Evolutionary Computation and Convergence to a Pareto Front," *Genetic Programming 1998 Conference*, 1998, pp. 221–228.

[30] Kumar, M., Husian, M., Upreti, N., and Gupta, D., "Genetic Algorithm: Review and Application," *International Journal of Information Technology and Knowledge Management*, Vol. 2, No. 2, 2010, pp. 451–454.

[31] Kennedy, J., and Eberhart, R., "Particle Swarm Optimization," *IEEE International Conference on Neural Networks*, 1995, pp. 1942–1948.

[32] Hassan, R., Cohanim, B., and de Weck, O., "A comparison of particle swarm optimization and the genetic algorithm," *1st AIAA multidisciplinary design optimization specialist conference*, American Institute of Aeronautics and Astronautics, Austin, TX, 2005.

[33] Coello Coello, C. A., Pulido, G. T., and Lechuga, M. S., "Handling Multiple Objectives With Particle Swarm Optimization," *IEEE Transactions on Evolutionary Computation*, Vol. 8, No. 3, 2004, pp. 256–279.

[34] Fourie, P. C., and Groenwold, A. A., "The particle swarm optimization algorithm in size and shape optimization," *Structural and Multidisciplinary Optimization*, Vol. 23, No. 4, 2002, pp. 259–267.

[35] Durillo, J. J., García-Nieto, J., Nebro, A. J., Coello Coello, C. A., Luna, F., and Alba, E., "Multi-Objective Particle Swarm Optimizers: An Experimental Comparison," *International Conference on Evolutionary Multi-Criterion Optimization*, 2009, pp. 495–509.

[36] Sierra, M. R., and Coello Coello, C. A., "Improving PSO-based Multi-Objective Optimization using Crowding, Mutation and e-Dominance," *International Conference on Evolutionary Multi-Criterion Optimization*, 2005, pp. 505–519.

[37] Zapotecas Martínez, S., and Coello Coello, C. A., "A multi-objective particle swarm optimizer based on decomposition," *Proceedings of the 13th annual conference on Genetic and evolutionary computation*, 2011, pp. 69–76.

[38] Landrum, E. J., and Babb, C. D., "Wind-Tunnel Force and Flow Visualization Data at Mach Numbers From 1.6 to 4.63 for a series of Bodies of Revolution at Angles of Attack From -4 ° to 60 °," Tech. rep., NASA Langley Research Center, Hampton, Virginia, 1979.

[39] Fuhrmann, H. D., Hildebrand, J., Lalicata, T., and Corporation, O. S., "Aerothermodynamic Overview , X-34," *Journal of Spacecraft and Rockets*, Vol. 36, No. 2, 1999, pp. 153–159.

[40] Brauckmann, G. J., "X-34 Vehicle Aerodynamic Characteristics," *Journal of Spacecraft and Rockets*, Vol. 36, No. 2, 1999, pp. 229–239.